Antimalarial target vulnerability of the putative *Plasmodium falciparum* methionine synthase

Nirut Leela [1], **Parichat Prommana** [2], **Sumalee Kamchonwongpaisan** [2], **Tana Taechalertpaisarn** [1], **Philip J Shaw** Corresp. [2]

[1] Department of Microbiology, Faculty of Science, Mahidol University, Bangkok, Bangkok, Thailand

[2] National Center for Genetic Engineering and Biotechnology (BIOTEC), National Science and Technology Development Agency, Pathum Thani, Pathum Thani, Thailand

Corresponding Author: Philip J Shaw
Email address: philip@biotec.or.th

Background. *Plasmodium falciparum* possesses a cobalamin-dependent methionine synthase (MS). MS is putatively encoded by the PF3D7_1233700 gene, which is orthologous and syntenic in *Plasmodium*. However, its vulnerability as an antimalarial target has not been assessed. **Methods.** We edited the PF3D7_1233700 and PF3D7_0417200 (dihydrofolate reductase-thymidylate synthase, DHFR-TS) genes and obtained transgenic *P. falciparum* parasites expressing epitope-tagged target proteins under the control of the *glmS* ribozyme. Conditional loss-of-function mutants were obtained by treating transgenic parasites with glucosamine. **Results.** DHFR-TS, but not MS mutants showed a significant proliferation defect over 96 h, suggesting that *P. falciparum* MS is not a vulnerable antimalarial target.

Antimalarial target vulnerability of the putative *Plasmodium falciparum* methionine synthase

Nirut Leela[1], Parichat Prommana[2], Sumalee Kamchonwongpaisan[2], Tana Taechalertpaisarn[1], Philip J. Shaw [2]

[1] Department of Microbiology, Faculty of Science, Mahidol University, Bangkok, Thailand

[2] National Center for Genetic Engineering and Biotechnology (BIOTEC), National Science and Technology Development Agency, Pathum Thani, Thailand

Corresponding Author:

Philip J. Shaw[1]

National Center for Genetic Engineering and Biotechnology (BIOTEC), National Science and Technology Development Agency, Pathum Thani, 12120, Thailand

Email address: philip@biotec.or.th

Abstract

Background.

Plasmodium falciparum possesses a cobalamin-dependent methionine synthase (MS). MS is putatively encoded by the PF3D7_1233700 gene, which is orthologous and syntenic in *Plasmodium*. However, its vulnerability as an antimalarial target has not been assessed.

Methods.

We edited the PF3D7_1233700 and PF3D7_0417200 (dihydrofolate reductase-thymidylate synthase, DHFR-TS) genes and obtained transgenic *P. falciparum* parasites expressing epitope-tagged target proteins under the control of the *glmS* ribozyme. Conditional loss-of-function mutants were obtained by treating transgenic parasites with glucosamine.

Results.

DHFR-TS, but not MS mutants showed a significant proliferation defect over 96 h, suggesting that *P. falciparum* MS is not a vulnerable antimalarial target.

Introduction

Malaria is a devastating parasitic disease. Between 2019 and 2021, an estimated additional 13.4 million cases were attributed to malaria control disruptions, chiefly the COVID-19 pandemic (World Health Organization, 2022). Infections with *Plasmodium falciparum* are responsible for most malaria cases, which are treated with artemisinin combination therapy (ACT). Artemisinin-resistant *P. falciparum* parasites are widespread throughout Southeast Asia, and partially resistant parasites have evolved independently in parts of Africa (World Health Organization, 2022), prompting the need for antimalarials against novel targets. Given that the current standard of care for malaria is a three-day ACT regimen, any new antimalarial must be similarly fast-acting. Fast-acting antimalarials inhibit the functions of essential, vulnerable targets (Forte et al., 2021). More than half of the protein-coding genes in *P. falciparum* are annotated as essential based on the criterion that disruption of the protein-coding region by transposon insertion is not tolerated (Zhang et al., 2018). However, the absence of transposon insertion is not definitive annotation of essentiality because of local variation in transposon

insertion efficiency. One possible example of this scenario is the PF3D7_1311700 (cyt c-2) gene, which lacks transposon insertions but was shown to be dispensable by targeted knockout (Espino-Sanchez et al., 2023).

Identifying vulnerable targets is challenging because some essential genes are non-vulnerable, including targets for which specific inhibitors with antimalarial activity are available, such as deoxyhypusine synthase (Aroonsri et al., 2019), Niemann-Pick Type C1-Related protein (Istvan et al., 2019), and plasmepsin V (Sleebs et al., 2014; Polino et al., 2020). Partial loss-of-function (LOF) mutants of these genes have latent proliferation defects, and in the case of plasmepsin V, a defect was observed after 96 h only in LOF mutants with greater than 90% knockdown of the wild-type level of expression (Polino et al., 2020). Antimalarial discovery efforts might be better focused on directly identifying vulnerable targets with alternative assays rather than proving essentiality, which may require laborious monitoring of proliferation in LOF mutants with varying degrees of knockdown and/or conditional knockout mutants over extended periods for non-vulnerable targets. We propose to define vulnerable targets for the purpose of assay development as genes for which a partial LOF mutant (with significant knockdown of about 50 to 90% reduction of the wild-type expression level) has an acute proliferation defect observable at 96 h or sooner.

In this study, we developed a target vulnerability assay for LOF mutants created with the *glmS* ribozyme tool (Prommana et al., 2013). To apply the tool, the gene of interest must be modified by DNA transfection. Proof of concept for the tool was previously demonstrated for the dihydrofolate reductase-thymidylate synthase (DHFR-TS) gene modified by single-crossover integration of transfected circular DNA (Prommana et al., 2013; Aroonsri et al., 2016). This transfection method has been superseded by the more efficient CRISPR-Cas9 gene editing

system (Ghorbal et al., 2014). We edited the DHFR-TS gene to assess whether the *glmS* ribozyme was functional in the context of an edited gene, particularly one with the 3′ coding region replaced with artificial recodonized sequence as a consequence of gene editing. In addition, the LOF mutant obtained with an edited DHFR-TS gene was used to validate the target vulnerability assay. DHFR-TS is a known vulnerable target that is inhibited by antifolate drugs such as pyrimethamine and P218 (Yuthavong et al., 2012), and LOF mutants of DHFR-TS show significant proliferation defects at 72 h or earlier (Prommana et al., 2013); (Aroonsri et al., 2019).

To search for new antimalarial targets, we propose testing LOF mutants of unexplored genes in target vulnerability assay. Methionine metabolic pathways contain several unexplored antimalarial targets. Methionine is an essential amino acid in *P. falciparum* that must be obtained from salvage because proliferation is markedly reduced in culture media lacking methionine (Divo et al., 1985; Marreiros et al., 2023). *P. falciparum* salvages methionine via the new permeation pathway and a neutral amino acid transporter (Cobbold, Martin & Kirk, 2011). In addition to protein synthesis, methionine is used as a cofactor to produce the essential metabolite S-adenosyl-l-methionine (SAM) by the SAM synthase (SAMS) enzyme. The methyl group from SAM is transferred to various acceptors by methyltransferases to form S-adenosyl-l-homocysteine (SAH). SAH is hydrolyzed to adenosine and l-homocysteine (Hcy) by the highly conserved enzyme S-adenosyl-l-homocysteine hydrolase (Tanaka et al., 2004). *P. falciparum* lacks key enzymes in the reverse transsulfuration pathway for the conversion of Hcy to cysteine. Consequently, Hcy accumulates and is effluxed from the parasite during intra-erythrocytic growth (Beri et al., 2017). However, excess Hcy is deleterious and can trigger gametocytogenesis in *P. falciparum* (Beri et al., 2017). In addition to efflux for the control of

Hcy, Hcy can be converted to methionine by the action of the methionine synthase enzyme (MS, 5-methyl tetrahydrofolate homocysteine methyltransferase, EC.2.1.1.13). MS uses 5-methyltetrahydrofolate (5-mTHF) as a cofactor to generate tetrahydrofolate (THF) as a by-product (Banerjee & Matthews, 1990). *P. falciparum* can obtain 5-mTHF from salvage or by synthesis from 5,10 methylenetetrahydrofolate via a methylenetetrahydrofolate reductase enzyme (Asawamahasakda & Yuthavong, 1993).

Cobalamin-dependent MS enzymatic activity was reported previously in *P. falciparum* intra-erythrocytic stage protein extract. Nitrous oxide inhibits the activity of this enzyme and parasite proliferation, suggesting that parasite cobalamin-dependent MS may be a potential antimalarial target (Krungkrai, Webster & Yuthavong, 1989). However, the gene encoding the parasite MS enzyme has not yet been identified in the *P. falciparum* 3D7 genome (Müller & Hyde, 2013). We identified a candidate *P. falciparum* MS gene and created a LOF mutant for assessing the vulnerability of this target.

Materials & Methods

Ethical approval

Blood for parasite culture was obtained by a protocol approved by the Ethics Committee, National Science and Technology Development Agency (NSTDA), Thailand, approval document #0021/2560. Written consent was obtained from all volunteers.

Bioinformatic analyses

The InterPro database (Paysan-Lafosse et al., 2023) was searched using the InterPro entry IPR003726 (Homocysteine-binding domain) via the InterPro web interface (https://www.ebi.ac.uk/interpro/). Protein sequences were obtained from UniProt (The UniProt Consortium et al., 2023) of the cobalamin-dependent methionine synthase (MS) enzymes from human (MTR, Q99707-1) and *Escherichia coli* K12 (metH, P13009), together with *Plasmodium* spp. candidate MS from orthologous group 1324at5820 encoded by *P. falciparum* PF3D7_1233700 (Pf, Q8I585), *P. knowlesi* PKH_145080 (Pk, A0A384KWI2), *P. malariae* PmUG01_14067900 (Pm, A0A1A8X239), *P. ovale wallikeri* PowCR01_140053700 (Pow, A0A1C3L5P3), *P. ovale curtisi* PocGH01_14059300 (Poc, A0A1D3UAH7), and *P. vivax* PVX_100640 (Pv, A0A1G4H5F2) genes. Sequences were aligned using the T-Coffee tool with default settings in the Expresso web interface (Armougom et al., 2006).

The X-ray structure determined to 1.90 Å resolution of the Hcy/5-mTHF binding fragment of *Thermotoga maritima* cobalamin-dependent MS co-complexed with Hcy and 5-mTHF (PDB: 1q8j; Evans et al., 2004) was used as a query for searching proteins with homologous structures in the *Plasmodium falciparum* 3D7 proteome. The PDB accession number was provided as a query source to the Foldseek web tool (Van Kempen et al., 2023; https://search.foldseek.com/search). Target search was restricted to the AlphaFold/Proteome v4 *P. falciparum* 3D7 database of 5,187 ab initio predicted protein structures using the 3Di/AA mode under default settings.

Construction of transfection vectors

Cas9 vectors were constructed by cloning oligonucleotides containing the guide RNA (gRNA) sequence (Table S1) into the pDC2-Cas9-hDHFRyFCU plasmid (Knuepfer et al., 2017)

digested with BbsI (New England Biolabs [NEB] Ipswich, MA, USA). To construct the repair vectors, we first made a mother plasmid (p3HA_glmS; Dataset S1) with *glmS* and HA elements to regulate and monitor the target protein, respectively. Repair vectors (Dataset S2 & S3) were constructed by simultaneous Gibson assembly cloning (NEB) of three synthetic fragments for each target (recodonized partial open reading frame, 5′ and 3′ HR) into the p3HA_glmS plasmid, linearized by digestion with KpnI (NEB). Recodonized coding region fragments were obtained as gBlocks synthetic DNA (IDT, Singapore). 5′ and 3′ HR fragments were obtained by PCR using PrimeSTAR® GXL DNA Polymerase (Takara Bio Inc. Shiga, Japan)) and *P. falciparum* 3D7 genomic DNA template.

Gene editing by DNA transfection

P. falciparum 3D7 reference (NCBI txid: 36329) wild-type parasite was cultured in vitro as previously described (Aroonsri et al., 2016; Aroonsri et al., 2019). Cas9 (20 µg) and PstI-linearized repair (50 µg) vectors were co-transfected into late schizont parasites by AMAXA nucleofection, as previously described (Knuepfer et al., 2017). WR99210 (2 nM, a gift from Prof. Tirayut Vilaivan) was applied 48 h post-transfection to select transfected parasites. WR99210-resistant parasites emerged within 30 days post-transfection, and gene editing events were detected by PCR with integration-specific primers (Table S1). Transfected parasites with detectable gene edits were treated for 7 days with 1 µM 5-fluorocytosine (Sigma-Aldrich, Merck KGaA, Germany) and 2.5 µg/mL blasticidin S HCl (Gibco™, Thermo Fischer Scientific, Waltham, MA, USA) to remove Cas9 plasmid retained as episome and eliminate wild-type parasites. Clonal lines of gene-edited parasites were obtained by limiting dilution in 96-well microtiter plates.

Western blotting

Clonal lines of transgenic parasites DHFR-TS_*glmS* and MS_*glmS* with edited PF3D7_0417200 and PF3D7_1233700 genes, respectively were synchronized by sorbitol treatment and cultured for 24 h in the presence or absence of 5 mM glucosamine (GlcN, Sigma-Aldrich). Parasites liberated from host cells by saponin treatment were lysed in RIPA Lysis and Extraction Buffer (Thermo Scientific, Thermo Fisher Scientific), sonicated for 15 s, and centrifuged at 14,000 g for 5 min. The supernatant was harvested, and the total protein concentration was determined by BCA protein assay (Pierce, Thermo Fisher Scientific). A sample of protein extract (50, 50, and 2.5 µg of total protein from 3D7 wild-type, MS_*glmS,* and DHFR-TS_*glmS* transgenic parasites, respectively) was separated in each lane of a NuPAGE 4–12% Bis-Tris protein gel in MOPS running buffer (Invitrogen, Thermo Fisher Scientific) using an XCell Surelock Electrophoresis cell (Invitrogen). Proteins were transferred onto a 0.45 µm PVDF transfer membrane (Thermo Scientific) by electroblotting using an XCell blot module (Invitrogen). The membrane was stained using LI-COR REVERT™ 700 total protein stain (LI-COR Biosciences, Lincoln, NE, USA). The membrane was blocked in Odyssey® blocking buffer (LI-COR Biosciences) overnight and probed with primary antibody (Anti-HA-Tag Rabbit Monoclonal antibody # SAB5600116, Sigma-Aldrich, diluted 1: 50,000) for 1 h. After washing three times, the membrane was incubated with IRDye 800CW goat anti-rabbit IgG (LI-COR Biosciences, diluted 1: 20,000) for 1 h. Blots were analyzed using the Odyssey® CLx Infrared Imaging System (LI-COR Biosciences). Total protein and target protein band (HA-tagged MS = 72.7 kDa and HA-tagged DHFR-TS = 75.5 kDa) intensities were determined using Image Studio v5.2 software (LI-COR Biosciences). Lane normalization factors were determined from the total

protein signal (700 nm channel) in each lane. The target protein band intensities (800 nm channel) were adjusted using the lane normalization factors. GlcN-treated lane-factor adjusted intensities were normalized to the corresponding signals of untreated parasites from the same experiment (100%), which were used for quantitative analysis. The % target protein (GlcN treated relative to untreated control) signals were analyzed using two-tailed one-sample Welch's *t*-tests in R Statistical Software (v4.3.0; R Core Team 2023), comparing the sample means with a null hypothesis mean of 100%. The *P*-values from *t*-statistics were adjusted using the Holm-Bonferroni post-hoc method in R. The mean DHFR-TS and MS % target protein signals were compared using two-tailed two-sample Welch's *t*-tests in R with the null hypothesis of no means difference.

Parasite proliferation (target vulnerability) assay

P. falciparum parasites were cultured for 96 h in 96-well microtiter plates at different GlcN concentrations. Parasite proliferation was assessed using SYBR Green I fluorescence as previously described (Aroonsri et al., 2016). The background-subtracted SYBR Green I signals from GlcN-treated parasites were normalized to the average background-subtracted signal from control parasites from the same synchronized culture without GlcN (100%) and were taken as response values for analysis. Data from at least three independent experiments for each parasite line were analysed using the drc package version 3.0-1 (Ritz & Streibig, 2005) in R v4.3.0 with the four-parameter log-logistic model. The top and bottom values were fixed at 100 and 0, respectively. The slope and 50% response (EC_{50}) values were fitted separately for each parasite line. EC_{50} values for each gene-edited transgenic line were compared with that of the 3D7 wild-

type strain using the EDcomp function in the drc R package. The *P*-values from *t*-statistics reported by EDcomp were adjusted using the Holm-Bonferroni post-hoc method in R.

Results

We hypothesized that *P. falciparum* possesses an MS-encoding gene. We searched for *P. falciparum* 3D7 proteins with an Hcy-binding domain in the InterPro database (Paysan-Lafosse et al., 2023), since all MS enzymes possess an N-terminal Hcy-binding domain (Matthews, Sheppard & Goulding, 1998). The PF3D7_1233700 gene product is the only *P. falciparum* 3D7 protein with an InterPro-annotated Hcy-binding domain. PF3D7_1233700 is annotated in OrthoDB (Kuznetsov et al., 2023) as a member of the syntenic *Plasmodium* orthologous group 1324at5820 (Hcy-binding domain). PF3D7_1233700 and orthologous (single-copy) proteins from other human-infective *Plasmodium* spp. showed low (≈20%) identity with human and *Escherichia coli* cobalamin-dependent MS (Fig. S1 & S2). We searched for candidate MS using a three-dimensional structural superposition-based approach (Foldseek), which is more sensitive for identifying homologous proteins (Van Kempen et al., 2023). Full-length cobalamin-dependent MS comprises four modules (N-terminal Hcy-binding, 5-mTHF-binding, cobalamin-binding, and C-terminal adenosylmethionine-binding/reactivation; Matthews, Sheppard & Goulding, 1998). The X-ray structures of cobalamin-dependent MS protein fragments from different species have been determined, although the structure of the N-terminal fragment containing Hcy- and 5-mTHF substrate binding domains is available only for *Thermotoga maritima* (Evans et al., 2004). We selected the structure of the *T. maritima* cobalamin-dependent MS fragment co-complexed with Hcy and 5-mTHF as a query for Foldseek. The top-ranked

Foldseek hit to *P. falciparum* 3D7 proteins was PF3D7_1233700. Lower-ranked hits had well-defined annotations unrelated to methionine metabolism, suggesting incidental structural similarity of protein folds with functions unrelated to MS (Table S2). Notwithstanding the possibility of even more diverged proteins not detectable by sequence- or structure-based homology, PF3D7_1233700 is putatively assigned as *P. falciparum* MS. However, definitive annotation requires direct functional data, e.g., biochemical assay of the purified PF3D7_1233700 protein for MS activity.

We edited the PF3D7_1233700 and PF3D7_0412700 (DHFR-TS) genes, placing them under the control of the *glmS* ribozyme (Prommana et al., 2013). The edited DHFR-TS and MS genes were confirmed by PCR genotypic assays in clonal lines of transgenic parasites (Fig. 1 & 2). One clonal line of each edited gene (designated as DHFR-TS_*glmS* and MS_*glmS*, respectively*)* was selected for phenotypic analysis. The expressions of target proteins in transgenic parasites were assessed by western blotting of synchronized transgenic parasites cultured for 24 h in the presence or absence of GlcN. Protein species of sizes expected for modified MS (72.7 kDa) and DHFR-TS (75.5 kDa) were detected in transgenic parasites (Fig. S3). GlcN treatment caused significant reductions in MS and DHFR-TS protein expression (DHFR-TS mean = 40%, *P*-adjusted=0.004; MS mean = 51%, *P*-adjusted=0.03; Fig. 3A). There was no significant difference in the mean % target protein (GlcN treated relative to untreated control) level between DHFR-TS and MS ($P = 0.34$).

Next, we assessed the consequences of target protein knockdown in transgenic parasites with respect to proliferation in target vulnerability assay. In previous studies of the acute effect of *glmS*-ribozyme mediated target knockdown on parasite proliferation, treatment was performed for up to 72 h in which GlcN has a minor inhibitory effect on wild-type strains (Prommana et al.,

2013). By extending the GlcN treatment to 96 h, greater than 50% inhibition of the 3D7 wild-type strain was observed at the highest concentrations such that we could determine the EC_{50} (8.0 mM; 95% confidence intervals 5.9 to 10.0 mM). We posited that knockdown of vulnerable target gene expression by the action of the *glmS* ribozyme enhances the proliferation defect caused by GlcN treatment itself over 96 h manifested as a significantly lower EC_{50} compared with 3D7 wild-type. The EC_{50} of the DHFR-TS_*glmS* parasite, but not that of the MS_*glmS* parasite, was significantly different from that of the 3D7 wild-type strain (Fig. 3B). Hence, reduction in DHFR-TS, but not MS expression affected parasite sensitivity to GlcN. Based on these results, DHFR-TS is defined as a vulnerable antimalarial target as expected. In contrast, MS is a non-vulnerable target.

Discussion

PF3D7_1233700 was identified as the only candidate gene encoding MS from a bioinformatic search of the *P. falciparum* 3D7 genome, suggesting that the parasite possesses a single MS gene. However, *P. falciparum* MS is not a vulnerable antimalarial target, in contrast to the vulnerability of the downstream SAMS enzyme in the *P. falciparum* methionine pathway (Musabyimana et al., 2022). Salvage is the major source of methionine substrate for *P. falciparum* SAMS because reducing exogenous methionine leads to a concomitant decrease of SAM (Harris et al., 2023). Hence, methionine synthesized by MS is of minor importance for intra-erythrocytic proliferation under standard in vitro culture conditions. However, methionine synthesis may be more important for *P. falciparum* proliferation in natural infections, since the methionine concentration in human serum (Barić et al., 2004) is approximately two to seven times lower than that of parasite culture medium.

The other roles of *P. falciparum* MS besides methionine synthesis should be considered to explain the conservation of MS in *Plasmodium* and its tentative annotation of essentiality in *P. falciparum* based on the absence of transposon insertions in the encoding gene (Zhang et al., 2018). It should be noted that definitive proof of essentiality requires demonstration of a proliferation defect from more complete knockdown using a different tool (e.g., the TetR-DOZI system with 5′ and 3′ aptamers installed at the target gene [Polino et al., 2020]) or from conditional gene knockout mutagenesis. Essential genes are expressed through the life cycle, and *P. falciparum* MS is detectably expressed by data-independent proteomics throughout the intraerythrocytic stages at a level approximately 40–1000-fold lower than that of DHFR-TS (Siddiqui et al., 2022). Moreover, single-cell RNA sequencing data indicate that *P. falciparum* MS is expressed during mosquito stages (Real et al 2021), and the *P. vivax* MS ortholog PVP01_1451800 is expressed in liver stages (Mancio-Silva et al 2022).

Although malaria parasites possess a mechanism for the efflux of Hcy (Beri et al., 2017), lack of MS function may lead to increased levels of Hcy and redox stress, which may be important for sporogonic development in the mosquito vector when *Plasmodium* is more dependent on glutathione (Vega-Rodríguez et al., 2009) and α-lipoic acid (Biddau et al., 2021) to mitigate oxidative stress. The conversion of 5-mTHF to THF by MS may be important for recycling folate required for other enzymatic reactions, particularly during the developmental stages with the greatest folate demand. *Plasmodium* can salvage folates and the folate precursor para-aminobenzoic acid (*p*ABA), but the levels of folates are too low, or are not in a form capable of being efficiently transported to support intra-erythrocytic development in the absence of de novo synthesis (Salcedo-Sora & Ward, 2013).

296 *P. berghei* lacking the *p*ABA synthetic enzyme aminodeoxychorismate synthase cannot
297 develop in *p*ABA-deficient medium during intraerythrocytic stages; however, the growth of
298 these mutant parasites is unaffected in *p*ABA-deficient medium during liver stages (Matz et al.,
299 2019). Despite an inefficient folate transport system for the uptake of 5-mTHF (Salcedo-Sora
300 and Ward, 2013), elevated levels of 5-mTHF in the liver may drive its accumulation and
301 conversion to THF by *Plasmodium* MS, such that the parasite is less reliant on de novo folate
302 synthesis during this stage of the life cycle. A knockout mutant of the *P. berghei* orthologous MS
303 gene (PBANKA_1448300) shows no growth defect during intraerythrocytic stages (Bushell et
304 al., 2017), but growth of the mutant is reduced during the transition from the sporozoite (through
305 the liver) to the blood stage (Stanway et al., 2019). Although these data suggest a non-essential
306 role of *Plasmodium* MS, dispensability in *P. falciparum* cannot be extrapolated from knockout
307 data in *P. berghei* because of species-specific differences in *Plasmodium* host cell tropism. *P.*
308 *berghei* preferentially invades reticulocytes, whereas *P. falciparum* invades mature erythrocytes.
309 The reticulocyte milieu has a greater metabolic complexity than that of erythrocytes, which can
310 support the growth of *P. berghei* parasites with knockouts of genes functioning in the
311 intermediary carbon metabolic pathway, pyrimidine metabolism, and glutathione biosynthesis
312 that are essential in *P. falciparum* (Srivastava et al., 2015).
313

314 Conclusions

315 The finding that MS is a non-vulnerable antimalarial target raises the question of what
316 other enzymes in the *Plasmodium* parasite methionine pathway and other pathways related to
317 folate metabolism (Müller and Hyde, 2013) are also non-vulnerable targets. This could be tested
318 by target vulnerability assay of LOF mutants for other genes annotated as essential. Although the

role of MS as an antimalarial target is deprioritized, it would be interesting to test whether the roles of *P. falciparum* MS in Hcy metabolism and folate recycling are more important in mosquito and liver stages.

Acknowledgments

We thank Prof. Tirayut Vilaivan (Chulalongkorn University, Bangkok, Thailand) for the gift of WR99210 and Dr. Ellen Knuepfer (Crick Institute, London, UK) for transfection plasmids and protocols.

References

Armougom F, Moretti S, Poirot O, Audic S, Dumas P, Schaeli B, Keduas V, Notredame C. 2006. Expresso: automatic incorporation of structural information in multiple sequence alignments using 3D-Coffee. *Nucleic Acids Research* 34:W604–W608. DOI: 10.1093/nar/gkl092.

Aroonsri A, Akinola O, Posayapisit N, Songsungthong W, Uthaipibull C, Kamchonwongpaisan S, Gbotosho GO, Yuthavong Y, Shaw PJ. 2016. Identifying antimalarial compounds targeting dihydrofolate reductase-thymidylate synthase (DHFR-TS) by chemogenomic profiling. *International Journal for Parasitology*. DOI: 10.1016/j.ijpara.2016.04.002.

Aroonsri A, Posayapisit N, Kongsee J, Siripan O, Vitsupakorn D, Utaida S, Uthaipibull C, Kamchonwongpaisan S, Shaw PJ. 2019. Validation of *Plasmodium falciparum* deoxyhypusine synthase as an antimalarial target. *PeerJ* 7:e6713. DOI: 10.7717/peerj.6713.

341 Asawamahasakda W, Yuthavong Y. 1993. The methionine synthesis cycle and salvage of
342 methyltetrahydrofolate from host red cells in the malaria parasite *(Plasmodium*
343 *falciparum)*. *Parasitology* 107:1–10. DOI: 10.1017/S0031182000079348.
344 Banerjee RV, Matthews RG. 1990. Cobalamin-dependent methionine synthase. *The FASEB*
345 *Journal* 4:1450–1459. DOI: 10.1096/fasebj.4.5.2407589.
346 Barić I, Fumić K, Glenn B, Ćuk M, Schulze A, Finkelstein JD, James SJ, Mejaški-Bošnjak V,
347 Pažanin L, Pogribny IP, Radoš M, Sarnavka V, Šćukanec-Špoljar M, Allen RH, Stabler
348 S, Uzelac L, Vugrek O, Wagner C, Zeisel S, Mudd SH. 2004. *S* -adenosylhomocysteine
349 hydrolase deficiency in a human: A genetic disorder of methionine metabolism.
350 *Proceedings of the National Academy of Sciences* 101:4234–4239. DOI:
351 10.1073/pnas.0400658101.
352 Beri D, Balan B, Chaubey S, Subramaniam S, Surendra B, Tatu U. 2017. A disrupted
353 transsulphuration pathway results in accumulation of redox metabolites and induction of
354 gametocytogenesis in malaria. *Scientific Reports* 7:40213. DOI: 10.1038/srep40213.
355 Biddau M, Santha Kumar TR, Henrich P, Laine LM, Blackburn GJ, Chokkathukalam A, Li T,
356 Lee Sim K, King L, Hoffman SL, Barrett MP, Coombs GH, McFadden GI, Fidock DA,
357 Müller S, Sheiner L. 2021. Plasmodium falciparum LipB mutants display altered redox
358 and carbon metabolism in asexual stages and cannot complete sporogony in Anopheles
359 mosquitoes. *International Journal for Parasitology* 51:441–453. DOI:
360 10.1016/j.ijpara.2020.10.011.
361 Bushell E, Gomes AR, Sanderson T, Anar B, Girling G, Herd C, Metcalf T, Modrzynska K,
362 Schwach F, Martin RE, Mather MW, McFadden GI, Parts L, Rutledge GG, Vaidya AB,
363 Wengelnik K, Rayner JC, Billker O. 2017. Functional Profiling of a Plasmodium

Genome Reveals an Abundance of Essential Genes. *Cell* 170:260-272.e8. DOI: 10.1016/j.cell.2017.06.030.

Cobbold SA, Martin RE, Kirk K. 2011. Methionine transport in the malaria parasite Plasmodium falciparum. *International Journal for Parasitology* 41:125–135. DOI: 10.1016/j.ijpara.2010.09.001.

Divo AA, Geary TG, Davis NL, Jensen JB. 1985. Nutritional Requirements of *Plasmodium falciparum* in Culture. I. Exogenously Supplied Dialyzable Components Necessary for Continuous Growth. *The Journal of Protozoology* 32:59–64. DOI: 10.1111/j.1550-7408.1985.tb03013.x.

Espino-Sanchez TJ, Wienkers H, Marvin RG, Nalder S, García-Guerrero AE, VanNatta PE, Jami-Alahmadi Y, Mixon Blackwell A, Whitby FG, Wohlschlegel JA, Kieber-Emmons MT, Hill CP, A. Sigala P. 2023. Direct tests of cytochrome *c* and c_1 functions in the electron transport chain of malaria parasites. *Proceedings of the National Academy of Sciences* 120:e2301047120. DOI: 10.1073/pnas.2301047120.

Evans JC, Huddler DP, Hilgers MT, Romanchuk G, Matthews RG, Ludwig ML. 2004. Structures of the N-terminal modules imply large domain motions during catalysis by methionine synthase. *Proceedings of the National Academy of Sciences* 101:3729–3736. DOI: 10.1073/pnas.0308082100.

Forte B, Ottilie S, Plater A, Campo B, Dechering KJ, Gamo FJ, Goldberg DE, Istvan ES, Lee M, Lukens AK, McNamara CW, Niles JC, Okombo J, Pasaje CFA, Siegel MG, Wirth D, Wyllie S, Fidock DA, Baragaña B, Winzeler EA, Gilbert IH. 2021. Prioritization of Molecular Targets for Antimalarial Drug Discovery. *ACS Infectious Diseases* 7:2764–2776. DOI: 10.1021/acsinfecdis.1c00322.

387 Ghorbal M, Gorman M, Macpherson CR, Martins RM, Scherf A, Lopez-Rubio J-J. 2014.
388 Genome editing in the human malaria parasite *Plasmodium falciparum* using the
389 CRISPR-Cas9 system. *Nature Biotechnology* 32:819–821. DOI: 10.1038/nbt.2925.
390 Harris CT, Tong X, Campelo R, Marreiros IM, Vanheer LN, Nahiyaan N, Zuzarte-Luís VA,
391 Deitsch KW, Mota MM, Rhee KY, Kafsack BFC. 2023. Sexual differentiation in human
392 malaria parasites is regulated by competition between phospholipid metabolism and
393 histone methylation. *Nature Microbiology*. DOI: 10.1038/s41564-023-01396-w.
394 Istvan ES, Das S, Bhatnagar S, Beck JR, Owen E, Llinas M, Ganesan SM, Niles JC, Winzeler E,
395 Vaidya AB, Goldberg DE. 2019. Plasmodium Niemann-Pick type C1-related protein is a
396 druggable target required for parasite membrane homeostasis. *eLife* 8:e40529. DOI:
397 10.7554/eLife.40529.
398 Knuepfer E, Napiorkowska M, van Ooij C, Holder AA. 2017. Generating conditional gene
399 knockouts in Plasmodium – a toolkit to produce stable DiCre recombinase-expressing
400 parasite lines using CRISPR/Cas9. *Scientific Reports* 7. DOI: 10.1038/s41598-017-
401 03984-3.
402 Krungkrai J, Webster HK, Yuthavong Y. 1989. Characterization of cobalamin-dependent
403 methionine synthase purified from the human malarial parasite, *Plasmodium falciparum*.
404 *Parasitology Research* 75:512–517. DOI: 10.1007/BF00931158.
405 Kuznetsov D, Tegenfeldt F, Manni M, Seppey M, Berkeley M, Kriventseva EV, Zdobnov EM.
406 2023. OrthoDB v11: annotation of orthologs in the widest sampling of organismal
407 diversity. *Nucleic Acids Research* 51:D445–D451. DOI: 10.1093/nar/gkac998.
408 Marreiros IM, Marques S, Parreira A, Mastrodomenico V, Mounce BC, Harris CT, Kafsack BF,
409 Billker O, Zuzarte-Luís V, Mota MM. 2023. A non-canonical sensing pathway mediates

Plasmodium adaptation to amino acid deficiency. *Communications Biology* 6:205. DOI: 10.1038/s42003-023-04566-y.

Matthews RG, Sheppard C, Goulding C. 1998. Methylenetetrahydrofolate reductase and methionine synthase: biochemistry and molecular biology. *European Journal of Pediatrics* 157:S54–S59. DOI: 10.1007/PL00014305.

Matz JM, Watanabe M, Falade M, Tohge T, Hoefgen R, Matuschewski K. 2019. Plasmodium Para-Aminobenzoate Synthesis and Salvage Resolve Avoidance of Folate Competition and Adaptation to Host Diet. *Cell Reports* 26:356-363.e4. DOI: 10.1016/j.celrep.2018.12.062.

Müller IB, Hyde JE. 2013. Folate metabolism in human malaria parasites—75 years on. *Molecular and Biochemical Parasitology* 188:63–77. DOI: 10.1016/j.molbiopara.2013.02.008.

Musabyimana JP, Distler U, Sassmannshausen J, Berks C, Manti J, Bennink S, Blaschke L, Burda P-C, Flammersfeld A, Tenzer S, Ngwa CJ, Pradel G. 2022. *Plasmodium falciparum* S-Adenosylmethionine Synthetase Is Essential for Parasite Survival through a Complex Interaction Network with Cytoplasmic and Nuclear Proteins. *Microorganisms* 10:1419. DOI: 10.3390/microorganisms10071419.

Paysan-Lafosse T, Blum M, Chuguransky S, Grego T, Pinto BL, Salazar GA, Bileschi ML, Bork P, Bridge A, Colwell L, Gough J, Haft DH, Letunić I, Marchler-Bauer A, Mi H, Natale DA, Orengo CA, Pandurangan AP, Rivoire C, Sigrist CJA, Sillitoe I, Thanki N, Thomas PD, Tosatto SCE, Wu CH, Bateman A. 2023. InterPro in 2022. *Nucleic Acids Research* 51:D418–D427. DOI: 10.1093/nar/gkac993.

Polino AJ, Nasamu AS, Niles JC, Goldberg DE. 2020. Assessment of Biological Role and Insight into Druggability of the *Plasmodium falciparum* Protease Plasmepsin V. *ACS Infectious Diseases* 6:738–746. DOI: 10.1021/acsinfecdis.9b00460.

Prommana P, Uthaipibull C, Wongsombat C, Kamchonwongpaisan S, Yuthavong Y, Knuepfer E, Holder AA, Shaw PJ. 2013. Inducible Knockdown of Plasmodium Gene Expression Using the glmS Ribozyme. *PLoS ONE* 8:e73783. DOI: 10.1371/journal.pone.0073783.

R Core Team. 2023. R: a language and environment for statistical computing. R Foundation for Statistical Computing, Vienna, Austria. Available at https://www.R-project.org/ (accessed 19 October 2023).

Ritz C, Streibig JC. 2005. Bioassay analysis using R. *Journal of Statistical Software* 12:1–22. DOI: 10.18637/jss.v012.i05.

Salcedo-Sora JE, Ward SA. 2013. The folate metabolic network of Falciparum malaria. *Molecular and Biochemical Parasitology* 188:51–62. DOI: 10.1016/j.molbiopara.2013.02.003.

Siddiqui G, De Paoli A, MacRaild CA, Sexton AE, Boulet C, Shah AD, Batty MB, Schittenhelm RB, Carvalho TG, Creek DJ. 2022. A new mass spectral library for high-coverage and reproducible analysis of the *Plasmodium falciparum* –infected red blood cell proteome. *GigaScience* 11:giac008. DOI: 10.1093/gigascience/giac008.

Sleebs BE, Lopaticki S, Marapana DS, O'Neill MT, Rajasekaran P, Gazdik M, Günther S, Whitehead LW, Lowes KN, Barfod L, Hviid L, Shaw PJ, Hodder AN, Smith BJ, Cowman AF, Boddey JA. 2014. Inhibition of Plasmepsin V Activity Demonstrates Its Essential Role in Protein Export, PfEMP1 Display, and Survival of Malaria Parasites. *PLoS Biology* 12:e1001897. DOI: 10.1371/journal.pbio.1001897.

455 Srivastava A, Creek DJ, Evans KJ, De Souza D, Schofield L, Müller S, Barrett MP, McConville
456 MJ, Waters AP. 2015. Host reticulocytes provide metabolic reservoirs that can be
457 exploited by malaria parasites. *PLoS pathogens* 11:e1004882. DOI:
458 10.1371/journal.ppat.1004882.
459 Stanway RR, Bushell E, Chiappino-Pepe A, Roques M, Sanderson T, Franke-Fayard B, Caldelari
460 R, Golomingi M, Nyonda M, Pandey V, Schwach F, Chevalley S, Ramesar J, Metcalf T,
461 Herd C, Burda P-C, Rayner JC, Soldati-Favre D, Janse CJ, Hatzimanikatis V, Billker O,
462 Heussler VT. 2019. Genome-Scale Identification of Essential Metabolic Processes for
463 Targeting the Plasmodium Liver Stage. *Cell* 179:1112-1128.e26. DOI:
464 10.1016/j.cell.2019.10.030.
465 Tanaka N, Nakanishi M, Kusakabe Y, Shiraiwa K, Yabe S, Ito Y, Kitade Y, Nakamura KT.
466 2004. Crystal Structure of S-Adenosyl-l-Homocysteine Hydrolase from the Human
467 Malaria Parasite *Plasmodium falciparum*. *Journal of Molecular Biology* 343:1007–1017.
468 DOI: 10.1016/j.jmb.2004.08.104.
469 The UniProt Consortium, Bateman A, Martin M-J, Orchard S, Magrane M, Ahmad S, Alpi E,
470 Bowler-Barnett EH, Britto R, Bye-A-Jee H, Cukura A, Denny P, Dogan T, Ebenezer T,
471 Fan J, Garmiri P, Da Costa Gonzales LJ, Hatton-Ellis E, Hussein A, Ignatchenko A,
472 Insana G, Ishtiaq R, Joshi V, Jyothi D, Kandasaamy S, Lock A, Luciani A, Lugaric M,
473 Luo J, Lussi Y, MacDougall A, Madeira F, Mahmoudy M, Mishra A, Moulang K,
474 Nightingale A, Pundir S, Qi G, Raj S, Raposo P, Rice DL, Saidi R, Santos R, Speretta E,
475 Stephenson J, Totoo P, Turner E, Tyagi N, Vasudev P, Warner K, Watkins X, Zaru R,
476 Zellner H, Bridge AJ, Aimo L, Argoud-Puy G, Auchincloss AH, Axelsen KB, Bansal P,
477 Baratin D, Batista Neto TM, Blatter M-C, Bolleman JT, Boutet E, Breuza L, Gil BC,

478 Casals-Casas C, Echioukh KC, Coudert E, Cuche B, De Castro E, Estreicher A,
479 Famiglietti ML, Feuermann M, Gasteiger E, Gaudet P, Gehant S, Gerritsen V, Gos A,
480 Gruaz N, Hulo C, Hyka-Nouspikel N, Jungo F, Kerhornou A, Le Mercier P, Lieberherr
481 D, Masson P, Morgat A, Muthukrishnan V, Paesano S, Pedruzzi I, Pilbout S, Pourcel L,
482 Poux S, Pozzato M, Pruess M, Redaschi N, Rivoire C, Sigrist CJA, Sonesson K,
483 Sundaram S, Wu CH, Arighi CN, Arminski L, Chen C, Chen Y, Huang H, Laiho K,
484 McGarvey P, Natale DA, Ross K, Vinayaka CR, Wang Q, Wang Y, Zhang J. 2023.
485 UniProt: the Universal Protein Knowledgebase in 2023. *Nucleic Acids Research*
486 51:D523–D531. DOI: 10.1093/nar/gkac1052.
487 Van Kempen M, Kim SS, Tumescheit C, Mirdita M, Lee J, Gilchrist CLM, Söding J, Steinegger
488 M. 2023. Fast and accurate protein structure search with Foldseek. *Nature Biotechnology*.
489 DOI: 10.1038/s41587-023-01773-0.
490 Vega-Rodríguez J, Franke-Fayard B, Dinglasan RR, Janse CJ, Pastrana-Mena R, Waters AP,
491 Coppens I, Rodríguez-Orengo JF, Jacobs-Lorena M, Serrano AE. 2009. The Glutathione
492 Biosynthetic Pathway of Plasmodium Is Essential for Mosquito Transmission. *PLoS*
493 *Pathogens* 5:e1000302. DOI: 10.1371/journal.ppat.1000302.
494 World Health Organization. 2022. *World malaria report 2022*. Geneva: World Health
495 Organization. License CC BY-NC-SA 2.0 IGO.
496 Yuthavong Y, Tarnchompoo B, Vilaivan T, Chitnumsub P, Kamchonwongpaisan S, Charman
497 SA, McLennan DN, White KL, Vivas L, Bongard E, others. 2012. Malarial dihydrofolate
498 reductase as a paradigm for drug development against a resistance-compromised target.
499 *Proceedings of the National Academy of Sciences* 109:16823–16828.

500 Zhang M, Wang C, Otto TD, Oberstaller J, Liao X, Adapa SR, Udenze K, Bronner IF, Casandra
501 D, Mayho M, Brown J, Li S, Swanson J, Rayner JC, Jiang RHY, Adams JH. 2018.
502 Uncovering the essential genes of the human malaria parasite *Plasmodium falciparum* by
503 saturation mutagenesis. *Science* 360:eaap7847. DOI: 10.1126/science.aap7847.

504

Figure 1

PF3D7_0417200 (DHFR-TS) gene editing.

(A) Schematic of PF3D7_0417200 gene editing (drawn to scale). The location of the guide RNA target for mediating double-strand DNA break is indicated by the lightning bolt symbol. Repair vector (Dataset S2) elements are indicated by the colored boxes, including homologous regions in blue, recodonized protein coding region (Rec.) in magenta, triple hemagglutinin epitope tag (HA) in cyan, *glmS* ribozyme (*glmS*) in red, blasticidin S deaminase selectable marker gene (BSD) in orange, and *Plasmodium* transcriptional regulatory elements in teal. The locations and sizes of amplicons expected from PCR using primers DHFR_37 F (P1), DHFRTS_1558R (P2), and glmS_3R (P3) are indicated by black arrows. The structures of the PF3D7_0417200 gene before editing in parental reference strain 3D7 wild-type (3D7 WT) and after editing in transgenic (DHFR-TS_*glmS*) parasites are shown. **(B)** PCR products from genotypic assay separated in 0.8% agarose gel. Three clonal lines of transgenic parasites were isolated; DHFR-TS_*glmS* clone #1 was selected for phenotypic analysis. Lane M: 1kb+ DNA ladder (Invitrogen, sizes indicated on the left).

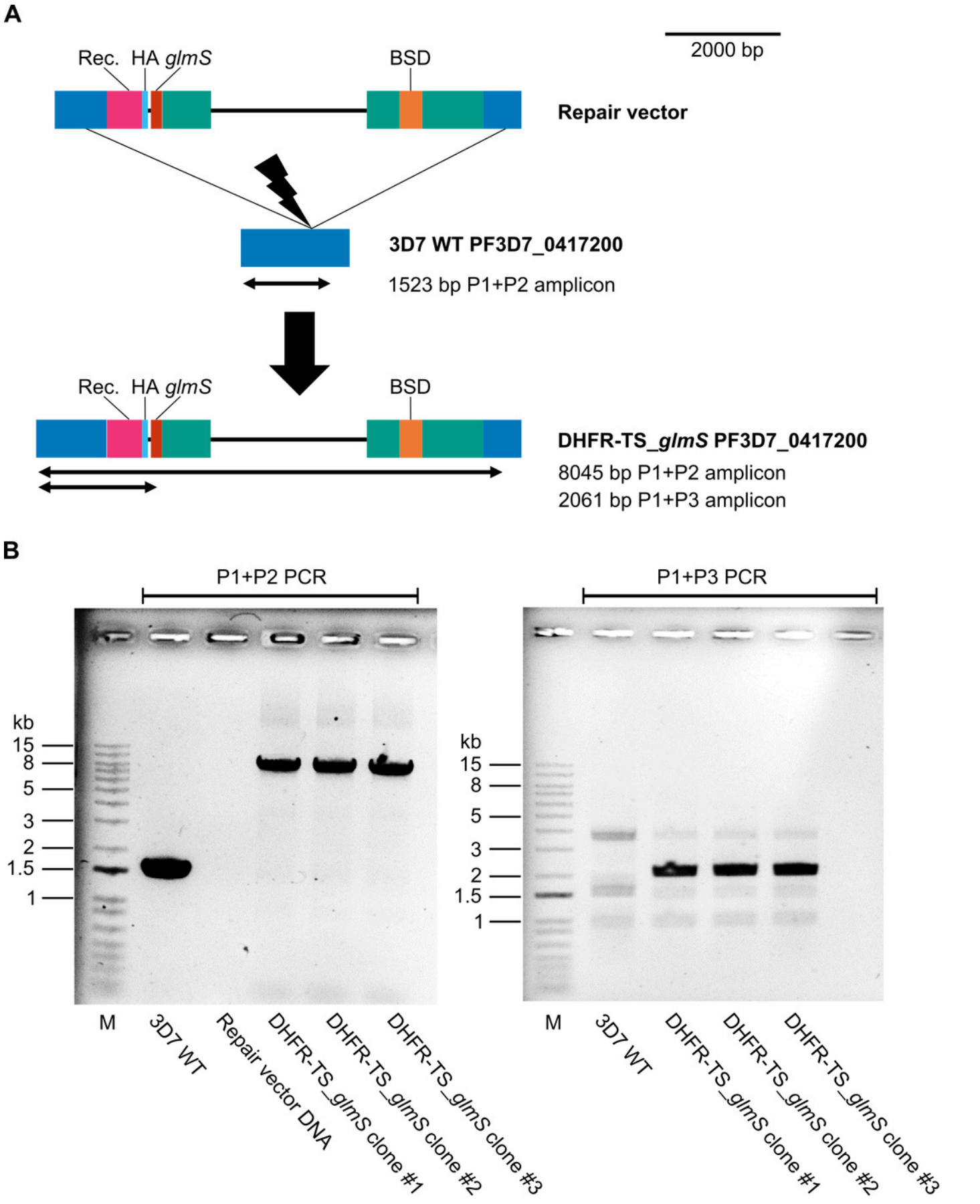
A
2000 bp
Rec. HA glmS
BSD
Repair vector
3D7 WT PF3D7_0417200
1523 bp P1+P2 amplicon
Rec. HA glmS
BSD
DHFR-TS_glmS PF3D7_0417200
8045 bp P1+P2 amplicon
2061 bp P1+P3 amplicon
B
P1+P2 PCR
P1+P3 PCR
kb
15
8
5
3
2
1.5
1
M
3D7 WT
Repair vector DNA
DHFR-TS_glmS clone #1
DHFR-TS_glmS clone #2
DHFR-TS_glmS clone #3

Figure 2

PF3D7_1233700 (MS) gene editing.

(A) Schematic of PF3D7_1233700 gene editing (drawn to scale). The location of the guide RNA target for mediating double-strand DNA break is indicated by the lightning bolt symbol. Repair vector (Dataset S3) elements are indicated by the colored boxes, including homologous regions in blue, recodonized protein coding region (Rec.) in magenta, triple hemagglutinin epitope tag (HA) in cyan, *glmS* ribozyme (*glmS*) in red, blasticidin S deaminase selectable marker gene (BSD) in orange, and *Plasmodium* transcriptional regulatory elements in teal. The locations and sizes of amplicons expected from PCR using primers MS_5IntF (P1), MS_HR2_rev (P2), glmS_3R (P3), and MS_5recodonR (P4) are indicated by black arrows. The structures of the PF3D7_1233700 gene before editing in parental reference strain 3D7 wild-type (3D7 WT) and after editing in transgenic (MS_*glmS*) parasites are shown. **(B)** PCR products from genotypic assay separated in 0.8% agarose gel. Two clonal lines of transgenic parasites were isolated; MS_*glmS* parasite clone #1 was selected for phenotypic analysis. Lane M: 1kb+ DNA ladder (Invitrogen, sizes indicated on the left).

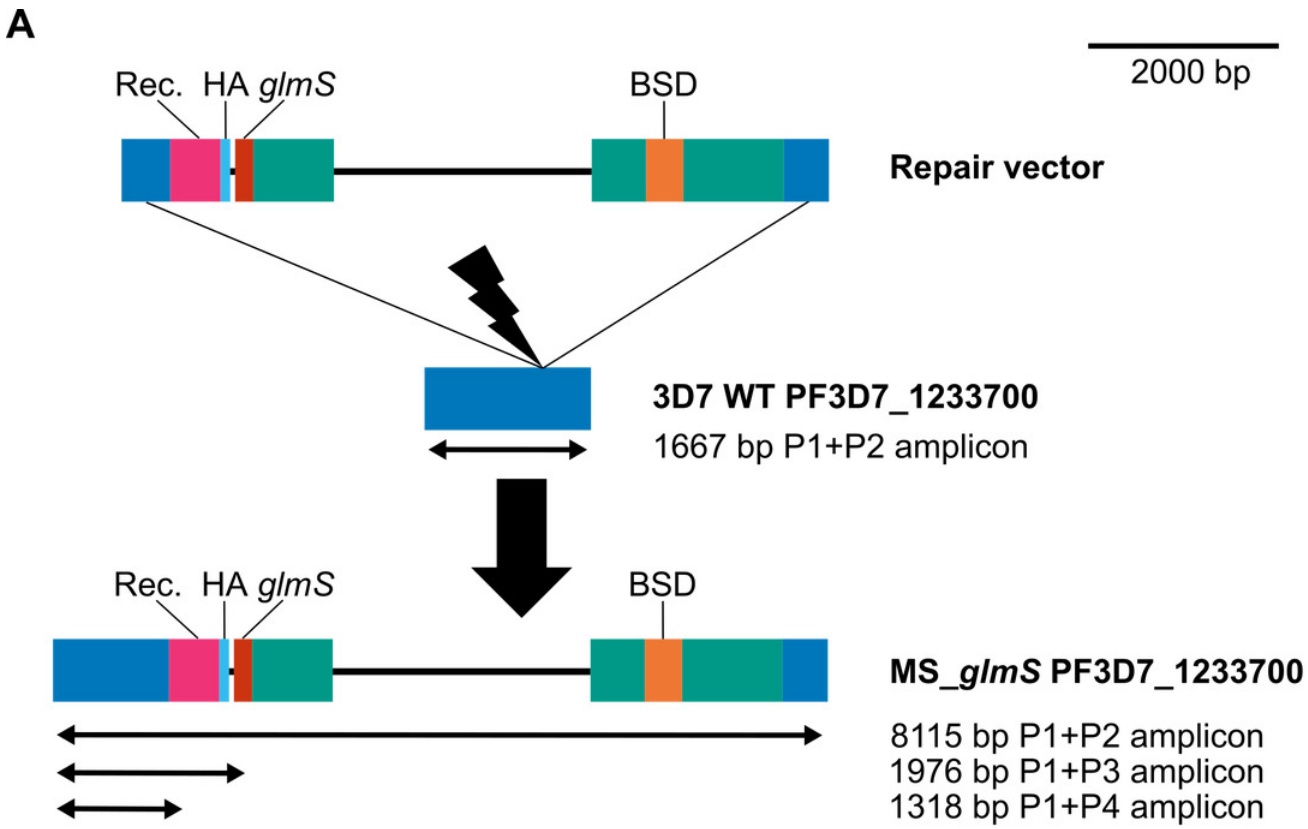
A
2000 bp
Rec. HA glmS
BSD
Repair vector
3D7 WT PF3D7_1233700
1667 bp P1+P2 amplicon
Rec. HA glmS
BSD
MS_glmS PF3D7_1233700
8115 bp P1+P2 amplicon
1976 bp P1+P3 amplicon
1318 bp P1+P4 amplicon

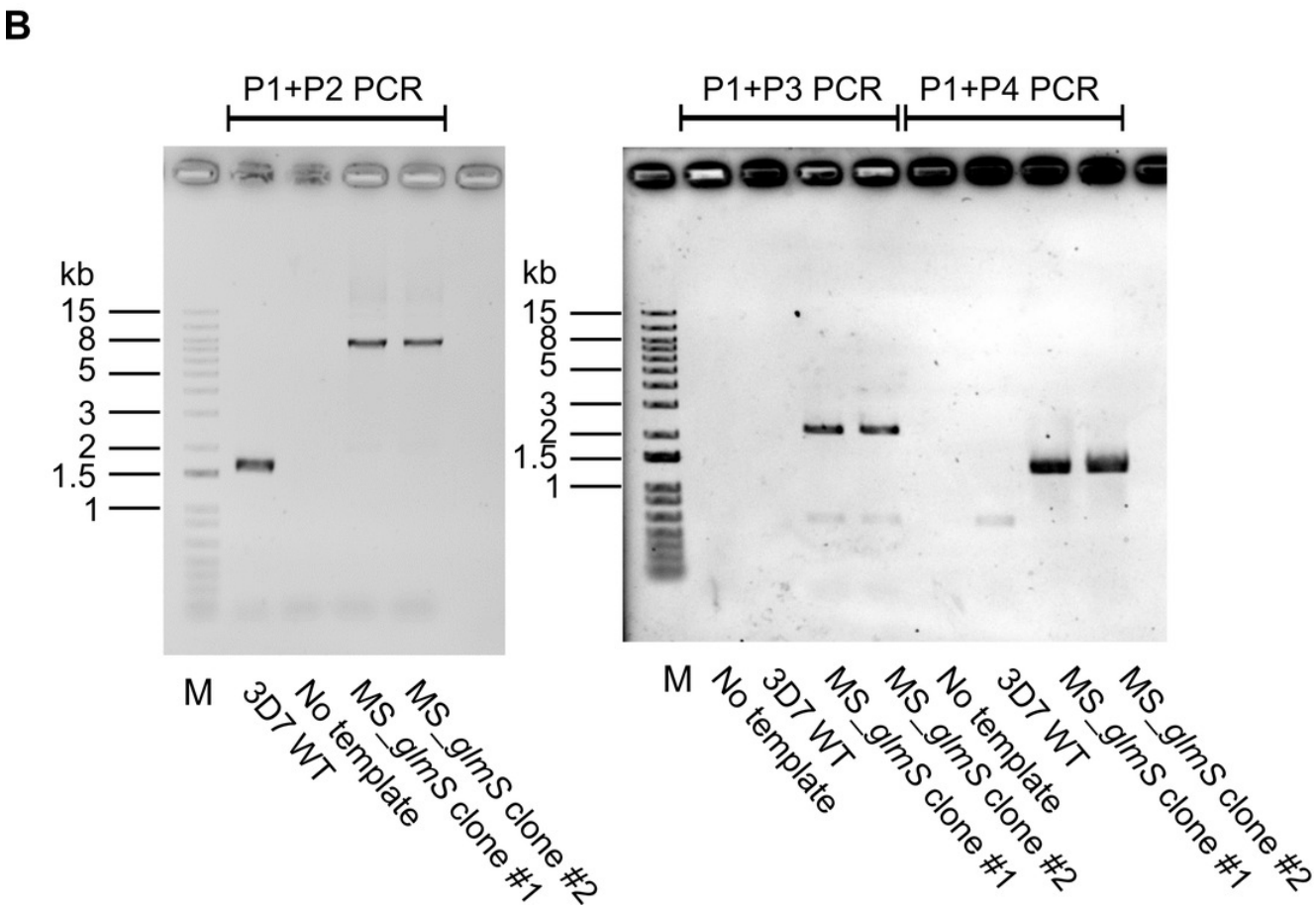
B
P1+P2 PCR
P1+P3 PCR
P1+P4 PCR
kb
15
8
5
3
2
1.5
1
M
3D7 WT
No template
MS_glmS clone #1
MS_glmS clone #2

Figure 3

Phenotypic analysis of gene-edited parasites.

In vitro cultures were established for *Plasmodium falciparum* reference 3D7 parental strain and transgenic parasite strains MS_*glmS* and DHFR-TS_*glmS* with edited PF3D7_1233700 (MS) and PF3D7_0417200 (DHFR-TS) genes, respectively. **(A)** Knockdown of target proteins in transgenic parasites. MS and DHFR-TS % target protein signals were obtained by western blotting (Fig. S3). Boxplots show the data from triplicate experiments. **(B)** Target vulnerability assay. Parasites were cultured for 96 h at different glucosamine (GlcN) concentrations. The left panel shows all data and model fits (curves). The right panel shows EC_{50} values for each transgenic line compared with that of the 3D7 parental strain. The points show the estimated EC_{50} ratio (3D7: transgenic parasite) and error bars represent S.E.M. The dashed line indicates the line of no effect. Estimated EC_{50} ratios:- 3D7: DHFR-TS_*glmS* = 11.25, adjusted *P*=7.9E-6; 3D7: MS_*glmS* = 0.89, adjusted *P*=0.84.

A

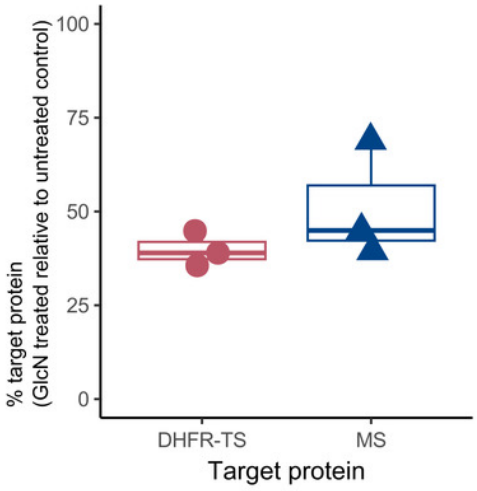
% target protein
(GlcN treated relative to untreated control)
100
75
50
25
0
DHFR-TS
MS
Target protein

B

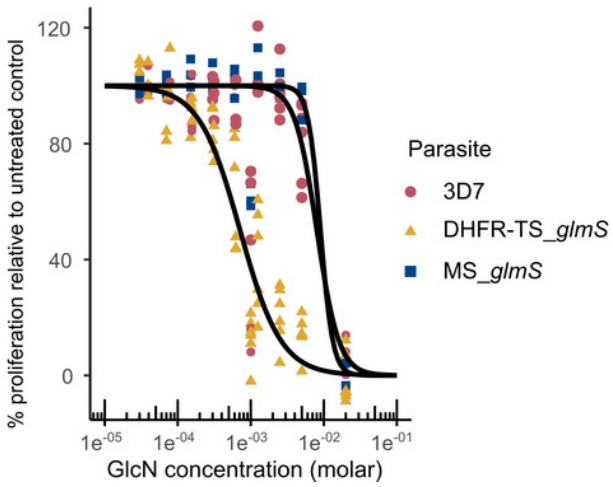
% proliferation relative to untreated control
120
80
40
0
1e-05
1e-04
1e-03
1e-02
1e-01
GlcN concentration (molar)
Parasite
3D7
DHFR-TS_glmS
MS_glmS

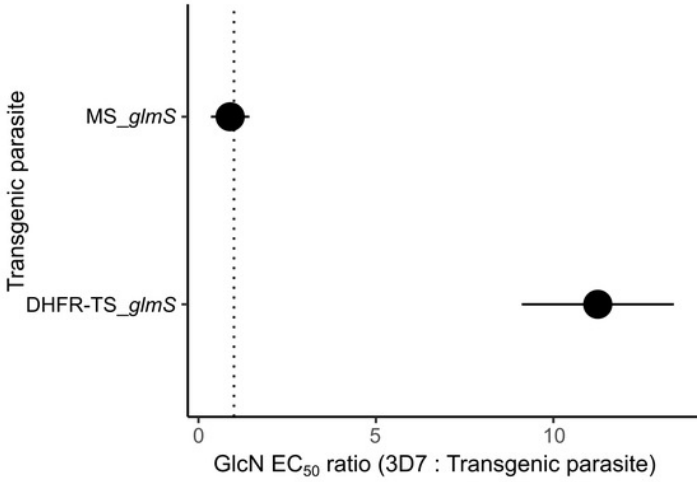
Transgenic parasite
MS_glmS
DHFR-TS_glmS
0
5
10
GlcN EC50 ratio (3D7 : Transgenic parasite)